Synthesis, PASS predication, *in vitro* antimicrobial evaluation and pharmacokinetic study of novel *n*-octyl glucopyranoside esters

Mohammed M. Matin, Sreebash C. Bhattacharjee, Priyanka Chakraborty, Muhammad S. Alam

PII: S0008-6215(19)30352-0

DOI: https://doi.org/10.1016/j.carres.2019.107812

Reference: CAR 107812

To appear in: *Carbohydrate Research*

Received Date: 5 June 2019

Revised Date: 30 August 2019

Accepted Date: 8 September 2019

Please cite this article as: M.M. Matin, S.C. Bhattacharjee, P. Chakraborty, M.S. Alam, Synthesis, PASS predication, *in vitro* antimicrobial evaluation and pharmacokinetic study of novel *n*-octyl glucopyranoside esters, *Carbohydrate Research* (2019), doi: https://doi.org/10.1016/j.carres.2019.107812.

Graphical abstract

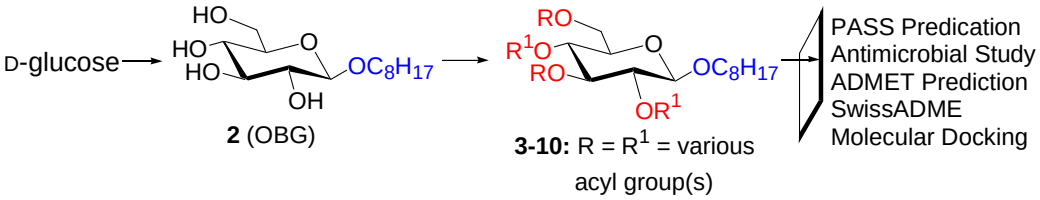

Synthesis, PASS Predication, *In Vitro* Antimicrobial Evaluation and Pharmacokinetic study of Novel *n*-Octyl Glucopyranoside Esters

Mohammed M. Matin,[a]* Sreebash C. Bhattacharjee,[a,b] Priyanka Chakraborty,[a] and Muhammad S. Alam[c]

[a]*Organic Research Laboratory, Department of Chemistry, Faculty of Science, University of Chittagong, Chittagong-4331, Bangladesh.*

[b]*Chemical Research Division, Bangladesh Council of Scientific & Industrial Research (BCSIR) Laboratories, Chittagong-4220, Bangladesh.*

[b]*Molecular Modeling and Drug Design Laboratory, Bangladesh Council of Scientific & Industrial Research (BCSIR) Laboratories, Chittagong-4220, Bangladesh.*

*Corresponding author. E-mail address: mahbubchem@cu.ac.bd, Tel.: +88 01716 839689.

Abstract

Octyl β-D-glucopyranoside (OBG), prepared from D-glucose and octan-1-ol employing MW method, was subjected to direct dimolar valeroylation in pyridine at room temperature (25 °C) with valeroyl chloride. This mainly furnished the corresponding 3,6-di-*O*-valeroate in 57% yield indicating the regioselectivity at C-6 and C-3 positions. For structural elucidation and to get newer glucopyranosides of potential antimicrobial 3,6-di-*O*-valeroate was further converted into four novel 2,4-di-*O*-acyl esters reasonably in good yields. Per-*O*-acetate and per-*O*-benzoate of OBG were also prepared for SAR study. PASS predication and *in vitro* antimicrobial studies established them as better antifungal agent than that of antibacterial. SAR study along with AdmetSAR and SwissADME suggested that incorporation of alkanoyl and aromatic ester groups on octyl glucopyranoside core increase antimicrobial potentiality in very low concentration (10 μgmL^{-1}). Molecular docking revealed that novel 2,4-di-*O*-tosyl ester and 2,3,4,6-tetra-*O*-benzoyl ester may act as competitive inhibitors of lanosterol 14-alpha demethylase.

Keywords

n-Octyl β-D-glucopyranoside (OBG); Regioselective acylation; PASS predication; Antimicrobial activities; AdmetSAR, SwissADME; Molecular docking.

1. Introduction

Carbohydrate fatty acid (CFA) esters especially selective acyl esters of monosaccharides containing both hydrophilic group and lipophilic group have synthetic utility as versatile intermediates in the syntheses of many natural products and their analogues which have a broad spectrum of applications [1]. These esters are biodegradable, nontoxic, nonallergic, nonionic surfactants and widely used in processed foods as stabilizing agents or emulsifiers [2]. However, selective acylation of monosaccharide molecules is a prominent challenge as monosaccharide molecules contain several hydroxyl groups (2°) of similar reactivity. These alcoholic groups compete during functionalization (esterification) step leading to a mono-, di- and polyesters [3]. Various methods have so far been developed and employed successfully for selective esterification (acylation) [4] such as direct method [5], protection-deprotection technique [6], organotin technique [7] etc. The latter two methods have many shortcomings such as increase the number of steps, tedious, expensive and hence generally decrease the overall yield. Enzyme catalyzed [8] and microwave (MW) assisted acylation [9] methods were also investigated in the past decade. In the case of enzymatic acylation of secondary hydroxyls of glycosides, the regioselectivity and yield of the reaction depends on many expensive factors [10] like the substrate must be able to bind in the active site of the enzyme [10b]. MW assisted esterification causes burning of sugars and selectivity is generally poor [9]. So, direct esterification method is preferred for selective acylation of monosaccharide molecules maintaining proper reaction conditions to reduce the number of steps [5c].

In recent years, the emergence of multiple antibiotic resistant pathogenic bacteria like methicillin-resistant *Staphylococcus aureus* (MRSA) is a global concern [11]. To combat with these organisms there is urgent need for establishment of new chemotherapeutic agents with novel mode of action. CFA esters have attracted considerable research interest and wide range of application in industry and medicine [12] due to their antimicrobial efficacy comparable to commercially available antimicrobials [13]. For example, in Japan sucrose esters of fatty acids [14] are used to reduce flat-sour spoilage due to *Bacillus* and *Clostridium* in canned coffee milk drinks [15]. In 2018, Chang *et al*. [16] reported regioselective synthesis of several monosaccharide esters for antimicrobial screening against a panel of bacteria and fungi. They identified 6-*O*-myristoyl-D-mannopyranose (**1**) as a lead compound which was highly active against methicillin resistant *Staphylococcus aureus* ATCC 33591 (MRSA) and can be used as an antimicrobial in food processing, preservation, and for bacterial and fungal diseases in animal and plants [16].

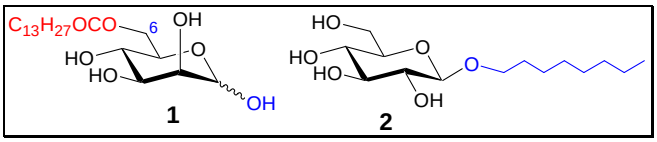

The antimicrobial property of CFA esters have been studied extensively, although variable results were reported for various bacterial and fungal species [17]. They can be both bacteriostatic and bactericidal [18]. Actually, antimicrobial functionality of CFA esters broadly depends on the carbohydrate core, degree of esterification and number and nature of fatty acid chain [19]. The sugar moieties present in CFA esters can increase drug water solubility, decrease toxicity and contribute to the bioactivity of the natural products. It is believed that CFA esters principally attack the cell membrane of bacteria [20] although exact mode of action is still unrevealed. Also, relatively a very few studies have examined the positional role of ester group(s) in the carbohydrate core for antimicrobial activity. Thus, it is very much reasonable to synthesize novel CFA esters and study their antimicrobial functionality with positional effect.

In the present study, several novel CFA esters were synthesized using *n*-octyl β-D-glucopyranoside (OBG, **2**) as the core carbohydrate moiety. Their antimicrobial efficacy was assessed against seven bacterial and five fungal strains. For structure activity relationship (SAR) study PASS (Prediction of Activity Spectra for Substances) predication and pharmacokinetic calculation (AdmetSAR, SwissADME) as well as molecular docking of these OBG esters were calculated and reported herein.

2. Results and discussion

*2.1. Synthesis of n-octyl β-D-glucopyranoside (OBG, **2**): Application of MW irradiation*

For the microwave assisted preparation of alkyl glycosides, generally, a mixture of sugar and alcohol is reacted in a high frequency field (2.45 GHz) in the presence of catalytic amount of an acid and the ratio of the α/β-anomers is influenced by the reaction conditions and reaction controlling [21]. Thus, we attempted for the synthesis of *n*-octyl β-D-glucopyranoside (OBG, **2**) using microwave irradiation (MWI). Thus, MWI of a mixture of D-glucose in anhydrous 1-octanol with Amberlite IR-120 (H^+) resin in a domestic microwave oven for 8 min at 180 watt (Scheme 1) followed by chromatography gave glycoside **2** along with octanol in good yield. However, to evaporate 1-octanol we used high temperature which reduces (due to burning) ultimate yield to 15% as solid mp 101-103 °C, lit. [22] mp 97-103 °C. In its ^{1}H NMR spectrum, additional seventeen protons was observed for octyl group and H-1 appeared as doublet with high coupling constant (7.8 Hz at δ 4.32 ppm) that requires diaxial relationship with H-2 proton. As H-1 is axially oriented octyloxy

group must be present equatorially leading to the formation of β-isomer and assigned as *n*-octyl β-D-glucopyranoside (OBG, **2**).

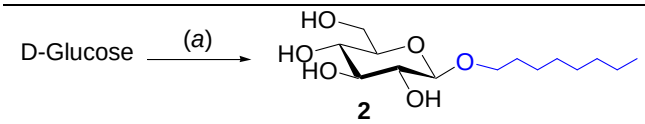

Scheme 1. *Reagents and conditions*: (*a*) 1-octanol, IR-120 (H^+) resin, MWI, 180 W, 30×16 sec, 15%.

*2.2. Regioselective valeroylation of OBG (**2**): Direct method*

OBG in hand, we carried out its dimolar valeroylation (pentanoylation) employing direct technique without any catalyst. Thus, treatment of OBG (**2**) with 2.1 equivalent of valeroyl chloride in dry pyridine at 0 °C for 1 h and 25 °C for 23 h showed the formation of two products (with little complex mixture, Scheme 2). Initial elution provided faster-moving component [R_f = 0.58 (*n*-hexane/EA = 2/1)] as a clear syrup in 11% yield.

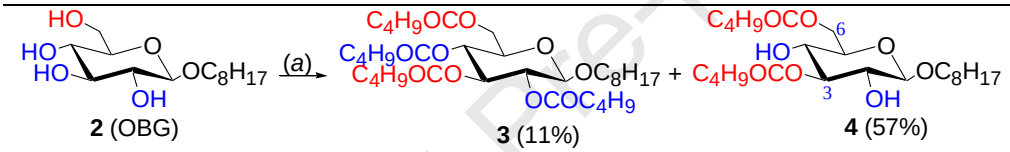

Scheme 2. *Reagents and conditions*: (*a*) C_4H_9COCl, dry Py, 0 °C-rt, 24 h.

Presence of four carbonyl signals and absence of OH band in its FT-IR spectrum indicated the complete valeroylation of the molecule. In the ^{1}H NMR spectrum, extra thirty-six protons appeared in the aliphatic region indicated the attachment of four valeroyloxy groups in the molecule. Also, H-2, H-3, H-4 and H-6 resonated in the considerable downfield as compared to its precursor compound **2** which confirmed the attachment of valeroyl groups at C-2, C-3, C-4 and C-6 positions. This is further supported by its ^{13}C NMR spectrum where four carbonyl peaks appeared at δ 173.4, 172.9, 172.1 and 172.0. Thus, the compound was assigned as *n*-octyl 2,3,4,6-tetra-*O*-valeroyl-β-D-glucopyranoside (**3**).

Further elution with *n*-hexane/EA (8/1) furnished the slower-moving component [R_f = 0.48 (*n*-hexane/EA = 2/1)] as a clear solid (57%), mp 62-65 °C (Scheme 2). Two ester carbonyl peaks at 1741 and 1733 cm^{-1} and a broad hydroxyl band at 3250-3540 cm^{-1} in its FT-IR spectrum clearly demonstrated the partial valeroylation of this compound. Its ^{1}H NMR spectrum exhibited extra eighteen protons at 2.46 (2H), 2.38 (2H), 1.55-1.70 (4H), 1.31-1.44 (4H) and 0.95 (6H) corresponding to two valeroyl groups. More importantly, H-3 and H-6 protons deshielded considerably at δ 5.07 (as t) and 4.48-4.42 (as dd), respectively as compared to its precursor OBG indicating the attachment of valeroyl groups at C-3 and C-6

positions. Its ^{13}C NMR spectrum displayed carbonyl peaks at δ 174.4 and 174.2. Other excess eight characteristic signals also appeared in the CH_2 and CH_3 region. On the basis of its spectral and elemental analyses, the compound was assigned as *n*-octyl 3,6-di-*O*-valeroyl-β-D-glucopyranoside (**4**). It should be noted that, structure of this compound was also confirmed by its conversion to its 2,4-di-*O*-acetate, which was well characterized by 1D and 2D NMR techniques and discussed in the next Section 2.3.

Isolation of **4** in low yield was probably due to the – (i) less selective reaction with comparatively smaller acylating agent like valeroyl chloride; (ii) less selective nucleophilic substitution reaction occurs at room temperature and (iii) formation of inseparable complex mixture of products. However, formation and isolation of 3,6-di-*O*-valeroate **4** and 2,3,4,6-tetra-*O*-valeroate **3** indicated the regiselectivity/reactivity order in OBG (**2**) under direct dimolar valeroylation at normal temperature is 6-OH > 3-OH > 4-OH,2-OH.

*2.3. Synthesis of 2,4-di-O-acylates of 3,6-di-O-valeroate **4**: Direct method*

Compound **4** has two free hydroxyl groups at C-2 and C-4 positions. To get newer glucopyranoside esters of potential activity we exploited these positions for the preparation of newer CFA esters using four different types of acylating agents. Initially, compound **4** was reacted with dimolar amount of acetic anhydride for 12 h and obtained an oil in excellent yield (Scheme 3). Its FT-IR spectrum didn't show any band corresponding to OH group(s) indicating the di-*O*-acetylation of the molecule. In the ^{1}H NMR spectrum of this compound, three three-proton triplets at δ 0.94, 0.91 and 0.88 were assigned for methyl protons of two $CH_3(CH_2)_3CO$ and one $CH_3(CH_2)_7O$ groups. Whereas, two three-proton singlets appeared at δ 2.03 and 2.04 were due to two acetyl methyl protons (2×$COCH_3$). The H-2 and H-4 protons resonated considerable downfield at δ 5.00 (as dd) and 5.09 (as t), respectively as compared to δ 3.83-3.93 and 3.46-3.59, respectively of its precursor 3,6-di-*O*-valeroate **4**. These downfield shifts of H-2 and H-4 protons were indicative of the attachment of acetyloxy groups at C-2 and C-4 position, respectively. In its ^{13}C NMR two acetyl carbonyl peaks appeared at δ 169.3 and 169.2, also, two acetyl methyl carbons resonated at δ 20.6 and 20.5. So, the structure of the acetate was assigned as *n*-octyl 2,4-di-*O*-acetyl-3,6-di-*O*-valeroyl-β-D-glucopyranoside (**5**).

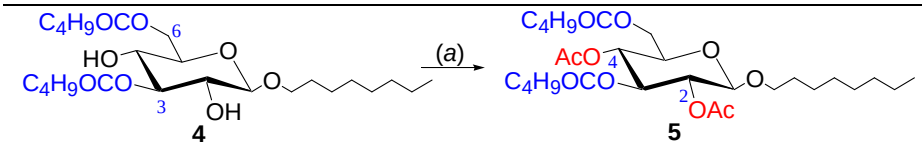

Scheme 3. *Reagents and conditions*: (*a*) Ac_2O, Py, 0 °C-rt, 12 h, 96%.

The assignments of the signals of this compound **5** were established by scanning and analyzing its DEPT-135, COSY, HSQC and HMBC experiments. In compound **5**, the position of two $COCH_3$ groups at C-2 and C-4 positions and two COC_4H_9 groups at C-3 and C-6 were ascertained by analyzing its HMBC experiment (Table 1 and Fig. 1-2).

Table 1. ^{1}H NMR and ^{13}C NMR shift values of compound **5**. ^{1}H and ^{13}C assignments were obtained from COSY, HSQC and HMBC experiments performed on Bruker DPX-400 spectrometer ($CDCl_3$).

Position	δ_H (ppm) (*J* Hz)	δ_C (ppm) (HSQC)	HMBC	COSY
1	4.50 (d, *J* = 8.0)	100.8	H: 2, 1’	H: 2
2	5.00 (dd, *J* = 9.6 & 8.0)	71.4	H: 1,4	H: 1.3
3	5.24 (t, *J* = 9.6)	72.5	-	H: 2,4
4	5.09 (t, *J* = 9.5)	68.6	H: 6	H: 3,5
5	3.68-3.73 (m)	71.9	H: 3	H: 4,6
6a,b	4.25 (dd, *J* = 12.4 & 4.8, 6a); 4.42 (dd, *J* = 12.4 & 2.4, 6b)	61.9	H: 4	H: 5
$1'_{A,B}$	3.88 (dt, *J* = 9.6 & 6.4, $1'_A$); 3.49 [dt, *J* = 9.6 & 6.9, $1'_B$)	70.2	H: 1	H: 2’
2′	1.51-1.68 (m)	-	-	H: 1’,3’
2- **CO**CH_3	2.03 (s)	169.2	H: 2, CO**CH_3**	-
3- **CO**C_4H_9	-	173.1	H: 3, CH_2	-
4- **CO**CH_3	2.04 (s)	169.3	H: 4, CO**CH_3**	-
6- **CO**C_4H_9	-	173.5	H: 6a,b, CH_2	-

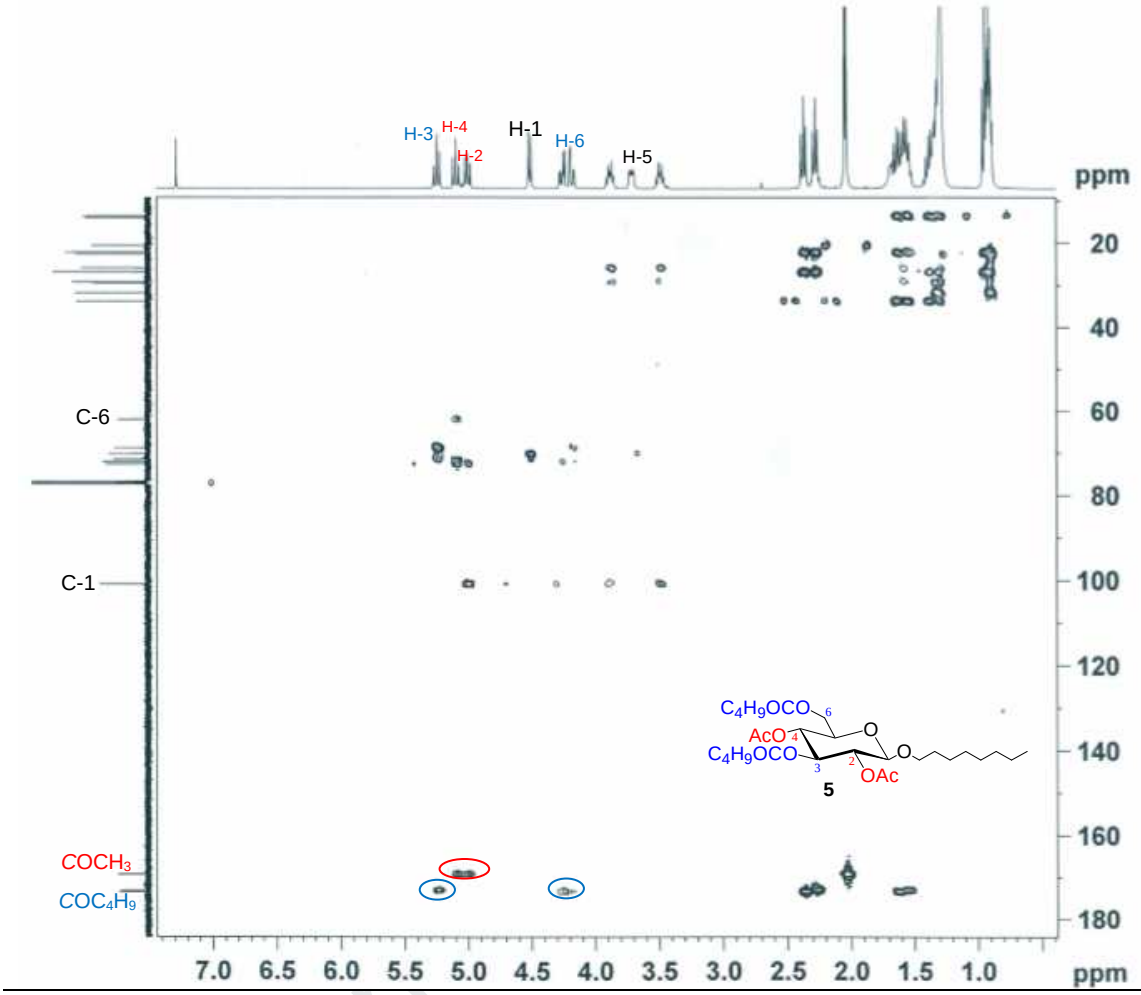

Fig. 1. 2D HMBC ($CDCl_3$) spectrum of compound **5**.

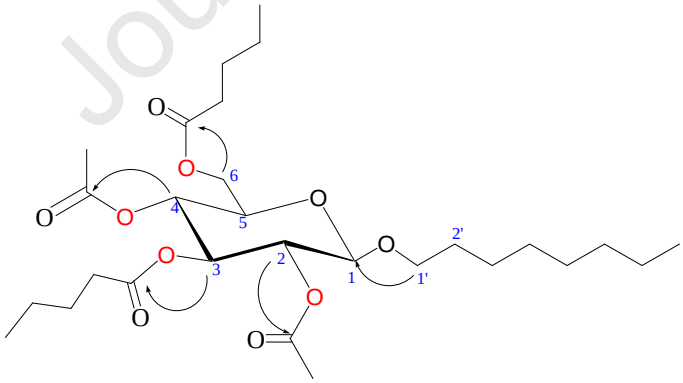

Fig. 2. The HMBC correlations for compound **5**.

Encouraged by these successes we used more three acylating agents for derivatization of valeroate **4**. Thus, reaction of valeroate **4** with dimolar decanoyl chloride, benzoyl chloride and tosyl chloride separately followed by purification furnished 2,4-di-*O*-decanoate **6**, 2,4-di-*O*-benzoate **7**, and 2,4-di-*O*-tosylate **8**, respectively in good yields (Scheme 4). All these compounds were characterized by FT-IR, ^{1}H, ^{13}C NMR and elemental analyses.

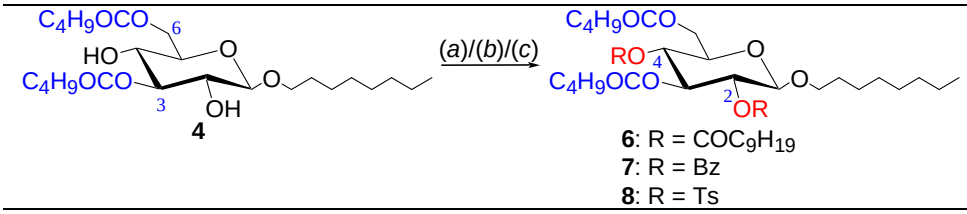

Scheme 4. *Reagents and conditions*: (*a*) $C_9H_{19}COCl$, Py, 0 °C-rt, 11 h, 45 °C, 1h, 76%; (*b*) C_6H_5COCl, Py, 0 °C-rt, 14 h, 82%; (*c*) 4-$CH_3.C_6H_4COCl$, Py, 0 °C-rt, 10 h, 78%.

*2.4. Synthesis of per-O-acyl esters of OBG (**2**): Direct method*

We have prepared two per-*O*-acyl esters of OBG (**2**) to get potential antimicrobial agents as well as to get idea about structure activity relationship (SAR) during antimicrobial activity evaluation. Initially, treatment of OBG (**2**) with excess amount of acetic anhydride in pyridine gave a faster-moving yellow solid, mp 58-60 °C in excellent yield (92%, Scheme 5). In its ^{1}H NMR spectrum, additional four three-proton singlets at δ 2.10, 2.06, 2.04 and 2.02 indicated the attachment of four acetyl groups in the molecule. The solid was unambiguously assigned the structure as *n*-octyl 2,3,4,6-tetra-*O*-acetyl-β-D-glucopyranoside (**9**) on the basis of spectral analyses.

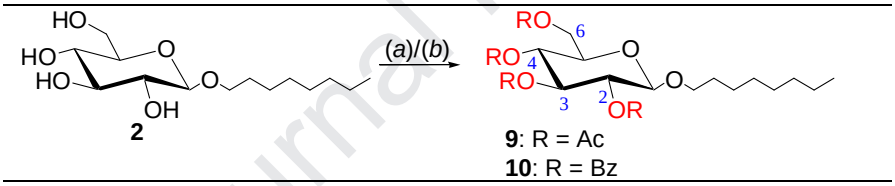

Scheme 5. *Reagents and conditions*: (*a*) Ac_2O, Py, 0 °C-rt, 12 h, 92%; (*b*) BzCl, dry Py, 0 °C-rt, 12 h, 87%.

Finally, OBG was treated with four equivalent of benzoyl chloride in pyridine and furnished a white solid, mp 97-100 °C in good yield (Scheme 5). FT-IR spectrum of this compound showed no signal related to OH group instead exhibited characteristic bands at 1723, 1719, 1715, 1710 (CO), 1069 cm^{-1} (pyranose ring). In the ^{1}H NMR spectrum, twenty protons resonated in the aromatic region which indicated the attachment of four benzoyl groups in the molecule. The solid was unambiguously assigned the structure as *n*-octyl 2,3,4,6-tetra-*O*-benzoyl-β-D-glucopyranoside (**10**).

Thus, we have successfully synthesized eight acyl esters of OBG using direct acylation technique with various acylating agents.

2.5. Computational antimicrobial activities evaluation: Prediction of Activity Spectra for Substances (PASS)

The web based application PASS predicts a plethora of pharmacological and toxicological activities of a compound simultaneously and the programme is designed to anticipate more than 4000 forms of biological activity including drug and non-drug actions and can be employed to identify the most probable targets with 90% accuracy [23]. PASS result is designated as Pa (probability for active compound) and Pi (probability for inactive compound). Being probabilities, the Pa and Pi values vary from 0.000 to 1.000. Only activities with Pa>Pi are considered as possible for a particular compound. If Pa>0.7, the chance to find the activity experimentally is high. When 0.5<Pa<0.7, the chance to find the activity experimentally is less, but the compound is probably not so similar to known pharmaceutical agents.

For the biological activity spectrum initially all the drugs was assigned SMILES (simplified molecular-input line-entry system). With these SMILES, biological activities were obtained by PASS online version (http://www.pharmaexpert.ru/ PASSonline/index.php). Predicted biological activities for OBG esters are mentioned in Table 2.

Table 2. Predicted biological activity of synthesized OBG esters using PASS online software.

Drug	Biological Activity			
	Antibacterial		Antifungal	
	Pa	Pi	Pa	Pi
2	0.533	0.014	0.685	0.010
3	0.544	0.013	0.705	0.009
4	0.563	0.011	0.738	0.008
5	0.567	0.011	0.725	0.009
6	0.544	0.013	0.705	0.009
7	0.532	0.014	0.703	0.009
8	0.404	0.029	0.537	0.025
9	0.563	0.011	0.716	0.009
10	0.494	0.017	0.653	0.013

Pa = Probability ‘to be active’; Pi = Probability ‘to be inactive’

Pa values of the OBG esters (**3-10**) were 0.40 < Pa < 0.56 in antibacterial and 0.53 < Pa < 0.73 in antifungal (Table 2), which indicated that the OBG esters should be more potent against phytopathogenic fungi as compared to that of bacterial pathogens.

2.6. In vitro antimicrobial evaluation of OBG esters

Knowing the possibility of antimicrobial efficacy of OBG esters from PASS predication we evaluated their activity *in vitro* against several bacterial and fungal strains.

*2.6.1. Effects of OBG esters **3-10** against bacteria*

In the present study, we used two Gram-positive and five Gram-negative organisms using disc diffusion method [24]. Gram-positive organisms were *Bacillus subtilis* ATCC 6633 and *Staphylococcus aureus* ATCC 25923. Five Gram-negative organisms were *Escherichia coli* ATCC 25922, *Escherichia coli* ATCC 8739, *Pseudomonas aeruginosa* ATCC 8027, *Pseudomonas aeruginosa* ATCC 27853 and *Salmonella abony* NCTC 6017.

2.6.1.1 Efficacy against Gram-positive organisms

The results of inhibition zone (diameter) of the selected bacteria due to the effect of synthesized glucoside type CFA esters are presented in Table 3 and Fig. 3. It was found from Table 3 that these esters were weak to moderate inhibitor against Gram-positive organisms.

Table 3. Inhibition against Gram-positive bacteria by the OBG esters.

Drug	Diameter of zone of inhibition in mm (10 µg dw / disc)	
	B. subtilis	*S. aureus*
2	2.41 ± 0.82	NI
3	6.54 ± 0.63	NI
4	4.62 ± 0.75	NI
5	*16.45±0.76	NI
6	NI	5.51 ± 0.44
7	5.55 ± 0.41	3.55 ± 0.41
8	*14.31 ± 0.82	2.41 ± 0.82
9	6.43 ± 0.82	5.64 ± 0.82
10	*21.43 ± 0.82	NI
Ciprofloxacin**	*27.71 ± 0.63	*35.22 ± 0.39

Data are presented as Mean ± SD. Values are represented for the triplicate of all the experiments. Significantly inhibition ($P < 0.05$) values are marked with asterisk (*) sign for test compounds and double asterisk (**) sign for reference antibiotic ciprofloxacin. dw = Dry weight; NI = No inhibition. NI was observed for control (DMSO).

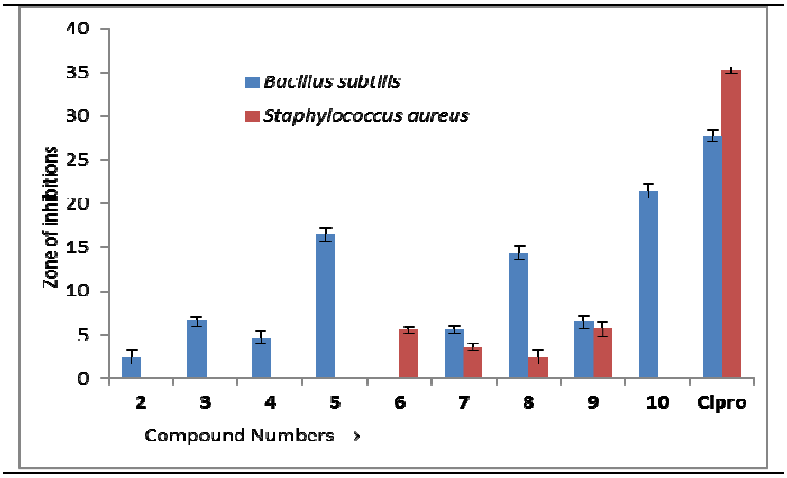

Fig. 3. Activities against Gram-positive organisms.

2.6.1.2 Efficacy against Gram-negative organisms

The results of inhibition zone (diameter) of the five selected bacteria due to the effect of synthesized OBG type CFA esters are presented in Table 4 and Fig. 4. It was clear from the Table 3 and Table 4 that OBG esters were less prone against these Gram-negative pathogens than Gram-positive strains.

Table 4. Inhibition against Gram-negative bacteria by the OBG esters.

Drug	Diameter of zone of inhibition in mm (10 µg dw / disc)				
	E. coli ATCC 25922	*E. coli* ATCC 8739	*P. aeruginosa* ATCC 8027	*P. aeruginosa* ATCC 27853	*S. abony* NCTC 6017
2	NI	NI	NI	NI	NI
3	8.22 ± 0.48	NI	NI	NI	9.56 ± 0.32
4	NI	12.23 ± 0.66	6.44 ± 0.68	10.50 ± 0.32	8.06 ± 0.72
5	NI	NI	NI	NI	NI
6	NI	12.66 ± 0.64	NI	NI	NI
7	12.56 ± 0.74	NI	NI	NI	9.22 ± 0.78
8	7.88 ± 0.56	NI	NI	NI	NI
9	NI	NI	NI	NI	8.22 ± 0.22
10	10.57 ± 0.82	NI	NI	NI	NI
Ciprofloxacin**	*31.65 ± 0.82	9.49 ± 0.44	14.55 ± 0.74	13.24 ± 0.42	12.20 ± 0.66

Data are presented as Mean ± SD. Values are represented for the triplicate of all the experiments. Significantly inhibition ($P < 0.05$) values are marked with asterisk (*) sign for test compounds and double asterisk (**) sign for reference antibiotic ciprofloxacin. dw = Dry weight; NI = No inhibition. NI was observed for control (DMSO).

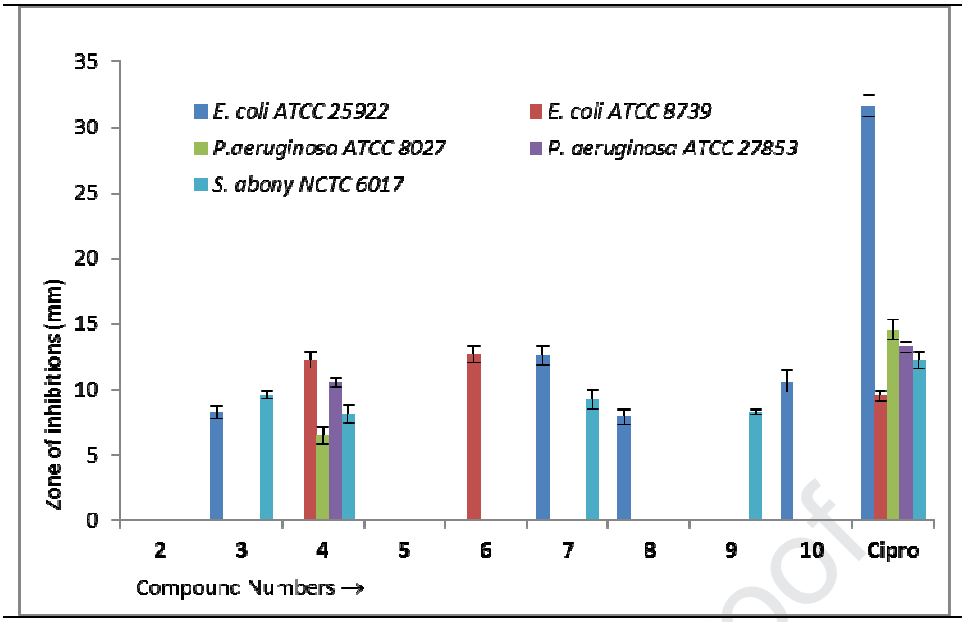

Fig. 4. Activities against Gram-negative organisms.

*2.6.2. Effects of OBG esters **3-10** against fungal pathogens*

The results of the percentage inhibitions of mycelial growth [25] due to the effect of the OBG esters **3-10** against four pathogenic fungi viz. *Aspergillus flavus*, *Aspergillus niger*, *Candida albicans* and *Fusarium solani* are presented in Table 5 and Fig. 5. It should be noted that OBG (**2**) didn't show any inhibition whereas introduction of ester groups at different position increased antifungal activities.

Table 5. Inhibition against fungal pathogens by the OBG esters.

Drug	% Inhibition of fungal mycelial growth (10 µg dw / mL PDA)			
	A. flavus	*A. niger*	*C. albicans*	*F. solani*
2	NI	NI	NI	NI
3	32.22 ± 0.44	*65.24 ± 0.42	*68.10 ± 0.82	*73.22 ± 0.64
4	NI	NI	34.74 ± 0.44	18.44 ± 0.72
5	35.36 ± 0.76	51.87 ± 0.68	53.26 ± 0.44	*64.86 ± 0.36
6	*65.67 ± 0.76	41.18 ± 0.72	*68.44 ± 0.82	*70.32 ± 0.58
7	25.83 ± 0.82	20.36 ± 0.34	NI	*71.89 ± 0.66
8	*62.50 ± 0.76	51.87 ± 0.82	*68.32 ± 0.76	*70.27 ± 0.68
9	*65.44 ± 0.42	18.12 ± 0.42	*68.39 ± 0.68	*73.68 ± 0.64
10	45.83 ± 0.44	*55.58 ± 0.60	*70.58 ± 0.60	*65.41 ± 0.68
**Fluconazole	*62.50 ± 0.66	17.11 ± 0.82	36.44 ± 0.68	*83.78 ± 0.46

Data are presented as Mean ± SD. Values are represented for the triplicate of all the experiments. Significantly inhibition ($P < 0.05$) values are marked with asterisk (*) sign for test compounds and double asterisk (**) sign for reference antibiotic fluconazole. dw = Dry weight; NI = No inhibition. NI was observed for control (DMSO).

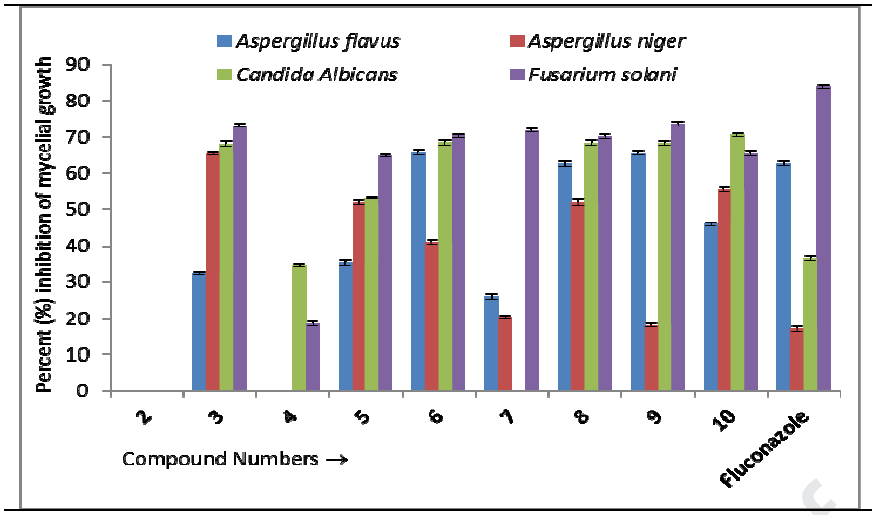

Fig. 5. Activities against fungal pathogens.

Most of the OBG esters, except **4**, possess antifungal potentiality against the tested pathogens. Their efficacy, in many cases is better than that of the standard antifungal fluconazole. OBG ester **3**, **6**, **8-10** showed excellent inhibition against *C. albicans* and **3**, **5-10** showed very good efficacy against *F. solani*.

More interestingly, *in vitro* results are in complete agreement with PASS predication result that the OBG esters were more potent against phytopathogenic fungi as compared to that of bacterial pathogens. Also, higher efficacy of **3**, **6** and **8-10** justified that the presence of aliphatic ester group and aromatic ester group in glucopyranoside molecular framework increase antimicrobial activities of OBG.

2.7. ADME/T analysis

From AdmetSAR calculation (Table 6), all the glucopyranoside derivatives, except **2**, showed positive result for blood brain barrier (BBB) criteria, predicting that they can pass through the BBB. They are non-carcinogenic (except **8**) and show III category acute oral toxicity which suggesting relatively harmless for oral administration. All compounds (except **2**) are P-glycoprotein inhibitor where, P-glycoprotein inhibition can interrupt the absorption, permeability and retention of the chemical species [26]. Amongst the OBG esters, compound **10** shows highest human intestinal absorption values whereas di-ester compound (**4**) showed the lowest value compared to others. Rat acute toxicity of OBG esters was found below 1.6 (mol/kg) (except **4** and **8)** which suggesting lower median lethal dose (LD_{50}) values. However, all the compounds show weak inhibitory feature for human ether-a-go-go-related gene (hERG) which can lead to long QT syndrome, so further more study of this aspect is necessary.

Table 6. AdmetSAR calculation of OBG esters.

Drug	Blood brain barrier	Human intestinal absorption	P-glycoprotein inhibitor	Human ether – a-go-go-related gene inhibition	Carcinogen	Acute oral toxicity	Rat acute toxicity LD_{50} (mol/kg)
2	- 0.5311	- 0.5967	NI (0.8709)	WI (0.8624)	NC (0.9490)	III	1.4828
3	+ 0.9392	+ 0.9106	I (0.6784)	WI (0.8839)	NC (0.8692)	III	1.6066
4	+ 0.5816	- 0.6026	I (0.7052)	WI (0.9357)	NC (0.9364)	III	2.0275
5	+ 0.9392	+ 0.9106	I (0.6784)	WI (0.8839)	NC (0.8692)	III	1.6066
6	+ 0.9392	+ 0.9106	I (0.6784)	WI (0.8839)	NC (0.8692)	III	1.6066
7	+ 0.9319	+ 0.9503	I (0.8893)	WI (0.8699)	NC (0.8755)	III	1.7512
8	+ 0.9120	+ 0.9449	I (0.7723)	WI (0.8203)	C (0.5550)	III	2.2737
9	+ 0.9392	+ 0.9106	I (0.6784)	WI (0.8839)	NC (0.8692)	III	1.6066
10	+ 0.9312	+ 0.9644	I (0.7430)	WI (0.8423)	NC (0.9149)	III	1.5788

NI = Non-inhibitor, I = Inhibitor, WI = Weak inhibitor, NC = Non-carcinogenic, C = Carcinogenic

From SwissADME calculation (Table 7), all the glucopyranoside derivatives have good hydrogen bonds donor and acceptor. According to Lipnski's rule of five poor absorption or permeation is more likely when there are more than 5 H-bond donors and 10 H-bond acceptors [27]. Topological polar surface area (TPSA) data showed the good polarity of the compounds, where the TPSA value should be less than 200 $Å^2$, More the value more the polarity. The CYP enzymes, particularly isoforms 1A2, 2C9, 2C19, 2D6, and 3A4, are responsible for about 90% oxidative metabolic reactions. Inhibition of CYP enzymes will lead to inductive or inhibitory failure of drug metabolism. Pan-assay interference compounds (PAINS) are chemical compounds that often give false positive results in high-throughput screens. PAINS tend to react nonspecifically with numerous biological targets rather than specifically affecting one desired target. Here PAINS showed no violation with these compounds.

Table 7. Calculation drug likeliness using SwissADME.

Drug	HB acceptors	HB donors	TPSA	CYP1A2 inhibitor	CYP2C19 inhibitor	CYP2C9 inhibitor	CYP2D6 inhibitor	CYP3A4 inhibitor	PAINS alerts
2	6	4	99.38	No	No	No	No	No	0
3	10	0	123.66	No	No	No	No	No	0
4	8	2	111.52	No	Yes	No	No	Yes	0
5	10	0	123.66	No	Yes	No	No	Yes	0
6	10	0	123.66	No	No	No	No	No	0
7	10	0	123.66	No	No	Yes	No	Yes	0
8	13	0	183.79	No	No	No	No	Yes	0
9	10	0	123.66	No	Yes	No	Yes	No	0
10	10	0	123.66	No	No	Yes	No	Yes	0

*HB = Hydrogen bond, TPSA = Topological polar surface area, PAINS = Pan-assay interference compounds

2.8. Molecular Docking and non-bond interaction analysis

In the present study, we tried to find a lanosterol 14-alpha demethylase inhibitor which play crucial role in ergosterol biosynthesis which ultimately causes rupture of cell membrane

[28]. Thus, we validated docking accuracy by redocking of a known ligand- itraconazole using XP docking methodology. The known co-crystal ligand was first separated and re-docked using the Glide XP algorithm. Conformation of the complex with the highest negative docking score was selected from each run. Interestingly, Glide docking with XP setting of ester **10** produced the docked complex with highest negative docking score, which denoted that the inhibitory ability of docked ligand was almost similar to that of the crystal, as shown in Table 8. Ester **10** and **8** showed glide docking score of -13.476 and -12.092 respectively where the known ligand itraconazole showed -12.296. The docked complexes of these two virtual hits from Glide XP docking were further analyzed for protein–ligand interaction profiling (Fig. 6). Tetrabenzoate **10** showed three carbon hydrogen bonds with ILE^{304} & $Gly^{307,}$ one hydrophobic pi-pi T-shaped with $TYR^{132,}$ one hydrophobic alkyl with ALA^{200} and seven hydrophobic pi-alkyl interactions with PHE475, PRO^{375}, ALA^{476}, LEU^{376}, MET^{508}, ILE^{131}, LYS^{143} & ILE^{304}.

On the other hand, compound **8** formed a conventional hydrogen bond with CYS^{470}, four carbon hydrogen bonds with LYS^{143}, GLY^{307} & HIS^{468}, thirteen hydrophobic alkyl bonds with LEU^{204}, ILE^{304}, LYS^{143}, LEU^{300}, ILE^{304}, ILE^{471}, LEU^{121}, MET^{508}, PRO^{375}, LEU^{376}, VAL^{509} and six hydrophobic pi-alkyl bonds with TYR^{118}, PHE^{233}, PHE^{475}, LEU^{376} and CYS^{470}. These all non-bond interactions revealed that novel ester **8** may act as competitive inhibitors of lanosterol 14-alpha demethylase.

Table 8. Glide docking of OBG ester **3**-**10**.

Drug	Glide XP docking score (kcal/mol)	Glide energy (kcal/mol)	Glide emodel (kcal/mol)	Glide ligand efficiency
10	-13.476	-71.39	-122.165	-0.259
itraconazole	-12.296	-75.401	-135.642	-0.196
8	-12.092	-67.215	-44.995	-0.228
4	-10.016	-57.222	-81.044	-0.313
7	-9.22	-76.162	-121.558	-0.192
5	-8.727	-61.135	-91.42	-0.23
3	-7.713	-61.154	-100.854	-0.175
2	-7.024	-41.932	-54.082	-0.351
9	-7.007	-50.074	-69.298	-0.219

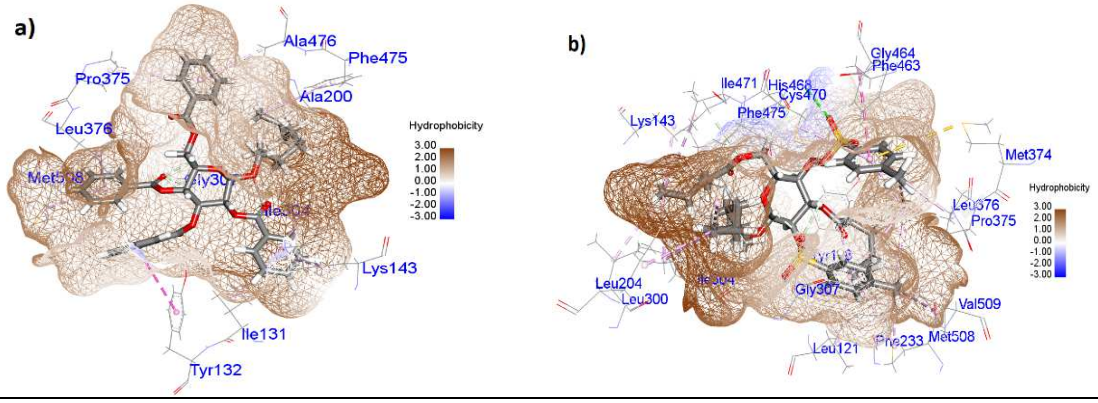

Fig. 6. Non-bond interactions of (a) compound **10** and (b) compound **8** with lanosterol 14-alpha demethylase.

3. Structure activity relationship (SAR)

It is essential to understand the mechanisms of antimicrobial action for the design and improvement of antimicrobial agents. Unlike antibiotics, CFA esters have diverse modes of action that appear to be nonspecific. Thus, we attempted to derive SAR of the OBG esters on the basis of our results. It was evident from Table 3 (Fig. 3), Table 4 (Fig. 4) and Table 5 (Fig. 5) that incorporation of valeroyl, decanoyl, benzoyl and tosyl groups, increased the antimicrobial potentiality of OBG (**2**).

Incorporation of valeroyl and other acyl group(s) gradually increased hydrophobicity of the OBG esters **4**, **3**, **5-10**. Previously we observed that the hydrophobicity of materials is an important parameter with respect to bioactivity such as toxicity or alteration of membrane integrity, because it is directly related to membrane permeation [29]. Hunt [30] also proposed that the potency of aliphatic alcohols is directly related to their lipid solubility through the hydrophobic interaction between alkyl chains from alcohols and lipid regions in the membrane. We believe that a similar hydrophobic interaction might occur between the acyl chains of glucopyranosides accumulated in the lipid like nature of the bacteria membranes. As a consequence of their hydrophobic interaction, bacteria lose their membrane permeability, ultimately causing death of the bacteria [30].

It was evident that, synthesized OBG esters **3-10** were more active against Gram-positive pathogen than that of Gram-negative bacterial organisms. More importantly, OBG esters **3-10** were highly prone against fungal pathogens than that of tested bacterial organisms.

4. Conclusion

Thus, dimolar valeroylation of OBG (**2**) at room temperature exhibited regioselectivity mainly at C-6 OH and C-3 OH positions confirming its reactivity order as 6OH > 3OH > 4OH,2OH. 3,6-Di-*O*-valeroylglucopyranoside, thus obtained, was then converted into four newer 2,4-di-*O*-acylates with other acylating agents. Also, per-*O*-acetate and per-*O*-

benzoates of OBG were prepared. Both PASS predication and *in vitro* antimicrobial activity test established that these OBG esters possess excellent antifungal activity as compared to antibacterial. SAR study demonstrated that for better antimicrobial activities aromatic moieties (phenyl ester) should be in combination with aliphatic acyl moieties. Parmacokinetic study such as AdmetSAR and SwissADME along with molecular docking of **8** and **10** are also discussed in connection with their drug likeliness. Overall, a very simple and effective direct acylation method is used to prepare several novel OBG esters (**3-8**) which have basically antifungal potentiality at a very low concentration (10 μgmL^{-1}).

5. Experimental

5.1. General methods

Evaporations were carried out under reduced pressure using a Buchi rotary evaporator (R-100, Switzerland) with a bath temperature below 40 °C. Melting points were determined on an electro-thermal melting point apparatus (England) and are uncorrected. Column chromatography was performed with silica gel G_{60}. Thin layer chromatography (TLC) was performed on Kieselgel GF_{254} and the spots were detected by spraying the plates with 1% H_2SO_4 and heating at 150–200 °C until coloration took place. The solvent system employed for the TLC analyses was chloroform/methanol and/or *n*-hexane/ethyl acetate in different proportions. FT-IR spectra were recorded on a FT-IR spectrophotometer (Shimadzu, IR Prestige-21) in KBr disc. ^1H (400 MHz, Bruker DPX-400 spectrometer, Switzerland) and ^{13}C (100 MHz) NMR spectra were recorded in $CDCl_3$ solution using tunable multinuclear probe. Chemical shifts were reported in δ unit (ppm) with reference to TMS as an internal standard and *J* values are shown in Hz. Elemental analyses were carried out with C,H-analyzer.

5.2. Synthesis

*5.2.1. Octyl β-D-glucopyranoside (**2**).* Amberlite IR-120 (H^+) resin (2.0 g) was added to a solution of D-glucose (1.0 g, 5.551 mmol) in anhydrous 1-octanol (20 mL) and the mixture was placed in a domestic microwave oven. The mixture was irradiated 30 sec span for sixteen times (i.e. 8 min) at 180 watt when TLC indicated completion of reaction with the formation of a faster-moving product. The resin was filtered off and the filtrate concentrated under reduced pressure. The resulting syrup was purified by passage through a silica gel column (with ethyl acetate/methanol, 8/1, v/v as eluant) to give the desired glycoside **2**. However, some octanol (bp ~195 °C) was present with glucoside **2**, which took our tedious effort (heating at 90-100 °C) to remove octanol and we obtained a little amount of

compound **2** (0.244 g, 15%) as a solid. Recrystallization from absolute ethanol gave the glucoside **2** as needles, mp 101-103 °C, lit. [22] mp 97-103 °C.

R_f = 0.51 (ethyl acetate/methanol = 2/1, v/v); FT-IR (KBr): ν 3200-3560 (OH), 1080 cm^{-1} (pyranose ring); ^{1}H NMR (400 MHz, $CDCl_3$): δ_H 4.32 (d, 1H, $J_{1,2}$ 7.8 Hz, H-1), 3.78-3.91 [br m, 7H, H-6, $CH_3(CH_2)_6CH_AH_BO$ and 4×O*H*], 3.63 (t, 1H, $J_{2,3;3,4}$ = 9.2 Hz, H-3), 3.50-3.57 [m, 2H, H-5 and $CH_3(CH_2)_6CH_AH_BO$], 3.39 (dd, 1H, H-2), 3.32 (t, 1H, $J_{4,5}$ 9.3 Hz, H-4), 1.61-1.68 [m, 2H, $CH_3(CH_2)_5CH_2CH_2O$], 1.22-1.37 [m, 10H, $CH_3(CH_2)_5CH_2CH_2O$], 0.90 [t, 3H, J 6.6 Hz, $CH_3(CH_2)_7O$]; ^{13}C NMR (100 MHz, $CDCl_3$): δ_C 102.8 (C-1), 76.4 (C-3), 75.5 (C-2), 73.4 (C-5), 70.6 [$CH_3(CH_2)_6CH_2O$], 69.5 (C-4), 61.4 (C-6), 31.8, 29.6, 29.5, 29.3, 25.9, 22.7 [$CH_3(CH_2)_6CH_2O$], 14.1 [$CH_3(CH_2)_7O$]; Anal. Calcd for $C_{14}H_{28}O_6$: C, 57.51; H, 9.65. Found: C, 57.62; H, 9.63.

*5.2.2. Octyl 2,3,4,6-tetra-O-valeroyl-β-D-glucopyranoside (**3**) and octyl 3,6-di-O-valeroyl-β-D-glucopyranoside (**4**).* A solution of octyl β-D-glucopyranoside (**2**, 0.5 g, 1.71 mmol) in pyridine (2 mL) was cooled to 0 °C whereupon valeroyl chloride (0.433 g, 3.591 mmol) was added to this mixture. The mixture was stirred at the same temperature for 1 h and then stirred 23 h at room temperature. TLC (*n*-hexane/EA, 1/2, v/v) indicated the formation of two products, the slower-moving component being the major one. Usual work-up followed by concentration gave a syrupy residue. During column chromatography, initial elution provided faster-moving component as 2,3,4,6-tetra-*O*-valeroate **3** (0.118 g, 11%) as a clear syrup.

R_f = 0.58 (*n*-hexane/EA = 2/1); FT-IR (KBr): ν 1756, 1752, 1750, 1733 (CO), 1090 cm^{-1} (pyranose ring); ^{1}H NMR (400 MHz, $CDCl_3$): δ_H 5.25 (t, 1H, $J_{3,4}$ 9.4 Hz, H-3), 5.11 (t, 1H, $J_{4,5}$ 9.6 Hz, H-4), 5.01 (1H, dd, $J_{2,3}$ 9.6 Hz, H-2), 4.50 (d, 1H, $J_{1,2}$ 8.0 Hz, H-1), 4.21 (dd, 1H, $J_{6a,6b}$ 12.1, $J_{5,6a}$ 4.8 Hz, H-6a), 4.18 (dd, 1H, $J_{5,6b}$ 2.0 Hz, H-6b), 3.87 [dt, 1H, J 9.6 and 6.4 Hz, $CH_3(CH_2)_6CH_AH_BO$], 3.66-3.72 (m, 1H, H-5), 3.47 [dt, 1H, J 9.6 and 6.8 Hz, $CH_3(CH_2)_6CH_AH_BO$], 2.36 [t, 2H, J 7.6 Hz, $CH_3(CH_2)_2CH_2CO$], 2.21-2.31 [m, 6H, 3×$CH_3(CH_2)_2CH_2CO$], 1.48-1.67 [m, 10H, $CH_3(CH_2)_5CH_2CH_2O$ and 4×$CH_3CH_2CH_2CH_2CO$], 1.26-1.40 [m, 18H, $CH_3(CH_2)_5(CH_2)_2O$ and 4×$CH_3CH_2(CH_2)_2CO$], 0.88-0.96 [m, 15H, $CH_3(CH_2)_7O$ and 4×$CH_3(CH_2)_3CO$]; ^{13}C NMR (100 MHz, $CDCl_3$): δ_C 173.4, 172.9, 172.1, 172.0 (*C*O), 100.9 (C-1), 72.5 (C-3), 72.0 (C-5), 71.2 (C-2), 70.1 [$CH_3(CH_2)_6CH_2O$], 68.4 (C-4), 62.0 (C-6), 33.8(2), 33.7(2) [4×$CH_3(CH_2)_2CH_2CO$], 31.8, 29.5, 29.3, 29.2, 27.0, 26.9, 26.8(2), 25.9, 22.6, 22.2(3), 22.1 [$CH_3(CH_2)_6CH_2O$ and 4×$CH_3(CH_2)_2CH_2CO$], 14.0 [$CH_3(CH_2)_7O$], 13.7, 13.6(2), 13.5

[4×*C*$H_3(CH_2)_3CO$]. Anal. Calcd for $C_{34}H_{60}O_{10}$: C, 64.94; H, 9.62. Found: C, 64.87; H, 9.65. Further elution with *n*-hexane/EA (8/1) furnished the 3,6-di-*O*-valeroate **4** (0.449 g, 57%) as a clear solid, mp 62-65 °C. R_f = 0.48 (*n*-hexane/EA = 2/1); FT-IR (KBr): ν 3250-3540 (OH), 1741, 1733 (CO), 1088 cm^{-1} (pyranose ring); ^{1}H NMR (400 MHz, $CDCl_3$): δ_H 5.07 (t, 1H, $J_{2,3;3,4}$ 9.6, H-3), 4.48 (dd, 1H, $J_{6a,6b}$ 12.1, $J_{5,6a}$ 4.5 Hz, H-6a), 4.42 (dd, 1H, $J_{5,6b}$ 2.0 Hz, H-6b), 4.34 (d, 1H, $J_{1,2}$ 8.2 Hz, H-1), 3.83-3.93 [m, 2H, H-2 and $CH_3(CH_2)_6CH_AH_BO$], 3.46-3.59 [m, 3H, H-4, H-5 and $CH_3(CH_2)_6CH_AH_BO$], 2.46 [t, 2H, J 7.7 Hz, $CH_3(CH_2)_2CH_2CO$], 2.38 [t, 2H, J 7.6 Hz, $CH_3(CH_2)_2CH_2CO$], 1.55-1.70 [m, 6H, $CH_3(CH_2)_5CH_2CH_2O$ and 2×$CH_3CH_2CH_2CH_2CO$], 1.31-1.44 [m, 14H, $CH_3(CH_2)_5CH_2CH_2O$ and 2×$CH_3CH_2(CH_2)_2CO$], 1.21-1.28 (br s, 2H, 2×OH), 0.95 [t, 6H, J 7.6 Hz, 2×$CH_3(CH_2)_3CO$], 0.89 [t, 3H, J 7.2 Hz, $CH_3(CH_2)_7O$]; ^{13}C NMR (100 MHz, $CDCl_3$): δ_C 174.4, 174.2 (*C*O), 101.0 (C-1), 74.3 (C-3), 74.2 (C-5), 71.1 (C-2), 70.4 [$CH_3(CH_2)_6CH_2O$), 69.4 (C-4), 63.0 (C-6), 34.1, 33.9 [2×$CH_3(CH_2)_2CH_2CO$], 31.8, 29.6, 29.3, 29.2, 27.0, 26.9, 25.9, 22.6, 22.2, 22.1 [$CH_3(CH_2)_6CH_2O$ and 2×$CH_3(CH_2)_2CH_2CO$], 14.0 [$CH_3(CH_2)_7O$], 13.6, 13.5 [2×$CH_3(CH_2)_3CO$]; Anal. Calcd for $C_{24}H_{44}O_8$: C, 62.58; H, 9.63. Found: C, 62.64; H, 9.61.

*5.2.3. General procedure for 2,4-di-O-acylation of compound **4** and 2,3,4,6-tetra-O-acylation of **2** by direct method.* To a solution of the **4** or **2** (0.1 g) in dry pyridine (1 mL) corresponding acyl halide (2.2 or 4.4 eq.) was added slowly at 0 ºC followed by addition of catalytic amount of DMAP. The reaction mixture was allowed to attain room temperature and stirring was continued for 11-18 h. For compounds **6** reaction mixture was stirred additional 1-2 h at 45 °C. A few pieces of ice was added to the reaction mixture to decompose excess acyl halide and extracted with DCM (5×3 mL). The DCM layer was washed successively with 5% hydrochloric acid, saturated aqueous sodium hydrogen carbonate solution and brine. The DCM layer was dried and concentrated under reduced pressure. The residue thus obtained on column chromatography (elution with *n*-hexane/ethyl acetate) gave the corresponding OBG esters.

*5.2.4. Octyl 2,4-di-O-acetyl-3,6-di-O-valeroyl-β-D-glucopyranoside (**5**):* Oil, yield 96%; R_f = 0.57 (*n*-hexane/EA = 2/1); FT-IR (KBr): ν 1761, 1760, 1733, 1729 (CO), 1091 cm^{-1} (pyranose ring); ^{1}H NMR (400 MHz, $CDCl_3$): δ_H 5.24 (t, 1H, $J_{3,4}$ 9.6 Hz, H-3), 5.09 (t, 1H, $J_{4,5}$ 9.5 Hz, H-4), 5.00 (dd, 1H, $J_{2,3}$ 9.6 Hz, H-2), 4.50 (d, 1H, $J_{1,2}$ 8.0 Hz, H-1), 4.25 (dd, 1H, $J_{6a,6b}$ 12.4, $J_{5,6a}$ 4.8 Hz, H-6a), 4.42 (dd, 1H, $J_{5,6b}$ 2.4 Hz, H-6b), 3.88 [dt, 1H, J 9.6 and 6.4 Hz, $CH_3(CH_2)_6CH_AH_BO$], 3.68-3.73 (m, 1H, H-5), 3.49 [dt, 1H, J 9.6 and 6.9 Hz, $CH_3(CH_2)_6CH_AH_BO$], 2.36 [t, 2H, J 7.6 Hz, $CH_3(CH_2)_2CH_2CO$], 2.27 [t, 2H, J 7.5 Hz,

$CH_3(CH_2)_2CH_2CO$], 2.04 (s, 3H, CH_3CO), 2.03 (s, 3H, CH_3CO), 1.51-1.68 [m, 6H, $CH_3(CH_2)_5CH_2CH_2O$ and $2\times CH_3CH_2CH_2CH_2CO$], 1.27-1.42 [m, 14H, $CH_3(CH_2)_5CH_2CH_2O$ and $2\times CH_3CH_2(CH_2)_2CO$], 0.94 [t, 3H, J 7.6 Hz, $CH_3(CH_2)_3CO$], 0.91 [t, 3H, J 7.6 Hz, $CH_3(CH_2)_3CO$], 0.88 [t, 3H, J 7.2 Hz, $CH_3(CH_2)_7O$]; ^{13}C NMR (100 MHz, $CDCl_3$): δ_C 173.5, 173.1, 169.3, 169.2 (*C*O), 100.8 (C-1), 72.5 (C-3), 71.9 (C-5), 71.4 (C-2), 70.2 [$CH_3(CH_2)_6CH_2O$], 68.6 (C-4), 61.9 (C-6), 33.8, 33.7 [$2\times CH_3(CH_2)_2CH_2CO$], 31.8, 29.4, 29.3, 29.2, 26.9, 26.8, 25.8, 22.6, 22.2, 22.1 [$CH_3(CH_2)_6CH_2O$ and $2\times CH_3(CH_2)_2CH_2CO$], 20.6, 20.5 ($CH_3CO$), 14.0 [$CH_3(CH_2)_7O$], 13.7, 13.5 [$2\times CH_3(CH_2)_3CO$]; Anal. Calcd for $C_{28}H_{48}O_{10}$: C, 61.74; H, 8.88. Found: C, 61.79; H, 8.86. The assignments of the signals of this compound **5** were established by scanning and analyzing its DEPT-135, COSY, HSQC and HMBC experiments.

*5.2.5. Octyl 2,4-di-O-decanoyl-3,6-di-O-valeroyl-β-D-glucopyranoside (**6**):* Oil, yield 76%; R_f = 0.65 (*n*-hexane/EA = 2/1); FT-IR (KBr): ν 1756, 1749, 1742, 1738 (CO), 1063 cm^{-1} (pyranose ring); ^{1}H NMR (400 MHz, $CDCl_3$): δ_H 5.23 (t, 1H, $J_{3,4}$ 9.6 Hz, H-3), 5.09 (t, 1H, $J_{4,5}$ 9.6 Hz, H-4), 5.00 (dd, 1H, $J_{2,3}$ 9.6 Hz, H-2), 4.48 (d, 1H, $J_{1,2}$ 8.0 Hz, H-1), 4.20 (dd, 1H, $J_{6a,6b}$ 12.2, $J_{5,6a}$ 4.8 Hz, H-6a), 4.16 (dd, 1H, $J_{5,6b}$ 2.0 Hz, H-6b), 3.85 [dt, 1H, J 9.6 and 6.4 Hz, $CH_3(CH_2)_6CH_AH_BO$], 3.66-3.71 (m, 1H, H-5), 3.45 [dt, 1H, J 9.6 and 6.8 Hz, $CH_3(CH_2)_6CH_AH_BO$], 2.42 [t, 2H, J 7.6 Hz, $CH_3(CH_2)_2CH_2CO$], 2.20-2.36 [m, 6H, $CH_3(CH_2)_2CH_2CO$ and $2\times CH_3(CH_2)_7CH_2CO$], 1.49-1.65 [m, 10H, $CH_3(CH_2)_5CH_2CH_2O$, $2\times CH_3CH_2CH_2CH_2CO$ and $2\times CH_3(CH_2)_6CH_2CH_2CO$], 1.21-1.39 [br m, 38H, $CH_3(CH_2)_5(CH_2)_2O$, $2\times CH_3CH_2(CH_2)_2CO$ and $2\times CH_3(CH_2)_6(CH_2)_2CO$], 0.87-0.95 [m, 15H, $CH_3(CH_2)_7O$, $2\times CH_3(CH_2)_3CO$ and $2\times CH_3(CH_2)_8CO$]; ^{13}C NMR (100 MHz, $CDCl_3$): δ_C 173.4, 172.9, 172.1, 172.0 (*C*O), 100.9 (C-1), 72.5 (C-3), 72.0 (C-5), 71.1 (C-2), 70.1 [$CH_3(CH_2)_6CH_2O$], 68.4 (C-4), 62.0 (C-6), 34.0(2), 33.8, 33.7 [$2\times CH_3(CH_2)_2CH_2CO$ and $2\times CH_3(CH_2)_7CH_2CO$], 31.8 (3) [$CH_3(CH_2)_5CH_2CH_2O$ and $2\times CH_3(CH_2)_6CH_2CH_2CO$], 30.0, 29.7, 29.4, 29.3(2), 29.2(3), 29.1, 29.0, 28.9, 28.7, 26.8(2), 25.9, 24.8, 24.7, 22.6(2), 22.2(2) [$CH_3(CH_2)_5CH_2CH_2O$, $2\times CH_3(CH_2)_2CH_2CO$ and $2\times CH_3(CH_2)_6(CH_2)_2CO$], 14.0(3), 13.6(2) [$CH_3(CH_2)_7O$, $2\times CH_3(CH_2)_3CO$ and $2\times CH_3(CH_2)_8CO$]; Anal. Calcd for $C_{44}H_{80}O_{10}$: C, 68.71; H, 10.48. Found: C, 68.69; H, 10.46.

*5.2.6. Octyl 2,4-di-O-benzoyl-3,6-di-O-valeroyl-β-D-glucopyranoside (**7**):* White solid, mp 62-65 °C, yield 83%; R_f = 0.60 (*n*-hexane/EA = 2/1); FT-IR (KBr): ν 1756, 1747, 1731, 1726 (CO), 1086 cm^{-1} (pyranose ring); ^{1}H NMR (400 MHz, $CDCl_3$): δ_H 8.03 (d, 2H, J 7.6 Hz, Ar-*H*), 7.99 (d, 2H, J 7.2 Hz, Ar-*H*), 7.56-7.64 (m, 2H, Ar-*H*), 7.45 (t, 4H, J 7.8 Hz, Ar-

H), 5.65 (t, 1H, $J_{3,4}$ 9.6 Hz, H-3), 5.43 (t, 1H, $J_{4,5}$ 9.6 Hz, H-4), 5.35 (dd, 1H, $J_{2,3}$ 9.6 Hz, H-2), 4.72 (d, 1H, $J_{1,2}$ 8.0 Hz, H-1), 4.27-4.32 (m, 2H, H-6), 3.88-3.97 (m, 2H, H-5 and $CH_3(CH_2)_6CH_AH_BO$], 3.48-3.55 [m, 1H, $CH_3(CH_2)_6CH_AH_BO$], 2.30 [t, 2H, J 7.2 Hz, $CH_3(CH_2)_2CH_2CO$], 2.09 [t, 2H, J 7.6 Hz, $CH_3(CH_2)_2CH_2CO$], 1.50-1.63 [m, 6H, $CH_3(CH_2)_5CH_2CH_2O$ and 2×$CH_3CH_2CH_2CH_2CO$], 1.08-1.26 [br m, 14H, $CH_3(CH_2)_5CH_2CH_2O$ and 2×$CH_3CH_2(CH_2)_2CO$], 0.92 [t, 6H, J 7.2 Hz, 2×$CH_3(CH_2)_3CO$], 0.85 [t, 3H, J 7.2 Hz, $CH_3(CH_2)_7O$]; ^{13}C NMR (100 MHz, $CDCl_3$): δ_C 173.4, 173.0 (C_4H_9CO), 165.1, 165.0 (PhCO), 133.5, 133.2, 129.9, 129.8, 129.5, 129.0, 128.5, 128.4 (Ar-*C*), 101.2 (C-1), 72.1 (C-3), 72.0 (C-5), 71.8 (C-2), 70.3 [$CH_3(CH_2)_6CH_2O$], 69.7 (C-4), 62.5 (C-6), 33.8, 33.7 [2×$CH_3(CH_2)_2CH_2CO$], 31.7 [$CH_3(CH_2)_5CH_2CH_2O$], 29.4, 29.2, 29.1 [$CH_3(CH_2)_2(CH_2)_3(CH_2)_2O$], 26.9, 26.8 [2×$CH_3CH_2CH_2CH_2CO$], 25.8 [$CH_3CH_2CH_2(CH_2)_5O$], 22.6 [$CH_3CH_2(CH_2)_6O$], 22.2, 21.9 [2×$CH_3CH_2(CH_2)_2CO$], 14.0 [$CH_3(CH_2)_7O$], 13.7, 13.3 [2×$CH_3(CH_2)_3CO$]; Anal. Calcd for $C_{38}H_{52}O_{10}$: C, 68.24; H, 7.84. Found: C, 68.31; H, 7.87.

*5.2.7. Octyl 2,4-di-O-tosyl-3,6-di-O-valeroyl-β-D-glucopyranoside (**8**):* Thick syrup, yield 78%; R_f = 0.51 (*n*-hexane/EA = 2/1); FT-IR (KBr): ν 1755, 1749 (CO), 1400 (br, SO_2), 1096 cm^{-1} (pyranose ring); ^{1}H NMR (400 MHz, $CDCl_3$): δ_H 7.82 (4H, d, *J* = 8.0 Hz, Ar-*H*), 7.31-7.39 (4H, m, Ar-*H*), 5.10-5.16 (m, 2H, H-3 and H-4), 4.82 (dd, 1H, $J_{2,3}$ 9.6 Hz, H-2), 4.34 (d, 1H, $J_{1,2}$ 8.0 Hz, H-1), 4.21 (dd, 1H, $J_{6a,6b}$ 12.4, $J_{5,6a}$ 5.2 Hz, H-6a), 4.17 (dd, 1H, $J_{5,6b}$ 2.0 Hz, H-6b), 3.87-3.92 [m, 1H, $CH_3(CH_2)_6CH_AH_BO$], 3.63-3.69 (m, 1H, H-5), 3.50-3.59 [m, 1H, $CH_3(CH_2)_6CH_AH_BO$], 2.52 (s, 3H, CH_3-C_6H_4), 2.48 (s, 3H, CH_3-C_6H_4), 2.28-2.47 [m, 4H, 2×$CH_3(CH_2)_2CH_2CO$], 1.55-1.63 [m, 6H, $CH_3(CH_2)_5CH_2CH_2O$ and 2×$CH_3CH_2CH_2CH_2CO$], 1.27-1.39 [br m, 14H, $CH_3(CH_2)_5CH_2CH_2O$ and 2×$CH_3CH_2(CH_2)_2CO$], 0.88-0.95 [m, 9H, $CH_3(CH_2)_7O$ and 2×$CH_3(CH_2)_3CO$]; Anal. Calcd for $C_{38}H_{56}O_{12}S_2$: C, 59.35; H, 7.34. Found: C, 59.34; H, 7.36.

*5.2.8. Octyl 2,3,4,6-tetra-O-acetyl-β-D-glucopyranoside (**9**):* Yellow solid, mp 58-60 °C, yield 92%; R_f = 0.56 (*n*-hexane/EA = 2/1); FT-IR (KBr): ν 1745, 1744, 1742, 1741 (CO), 1093 cm^{-1} (pyranose ring); ^{1}H NMR (400 MHz, $CDCl_3$): δ_H 5.22 (t, 1H, $J_{3,4}$ 9.5 Hz, H-3), 5.10 (t, 1H, $J_{4,5}$ 9.6 Hz, H-4), 5.00 (dd, 1H, $J_{2,3}$ 9.6 Hz, H-2), 4.50 (d, 1H, $J_{1,2}$ 8.0 Hz, H-1), 4.28 (dd, 1H, $J_{6a,6b}$ 12.4, $J_{5,6a}$ 4.8 Hz, H-6a), 4.15 (dd, 1H, $J_{5,6b}$ 2.0 Hz, H-6b), 3.88 [dt, 1H, J 9.6 and 6.4 Hz, $CH_3(CH_2)_6CH_AH_BO$], 3.67-3.72 (m, 1H, H-5), 3.49 [dt, 1H, J 9.6 and 6.8 Hz, $CH_3(CH_2)_6CH_AH_BO$], 2.10 (s, 3H, CH_3CO), 2.06 (s, 3H, CH_3CO), 2.04 (s, 3H, CH_3CO), 2.02 (s, 3H, CH_3CO), 1.53-1.62 [m, 2H, $CH_3(CH_2)_5CH_2CH_2O$], 1.22-1.36 [m, 10H, $CH_3(CH_2)_5CH_2CH_2O$], 0.90 [t, 3H, J 6.8 Hz, $CH_3(CH_2)_7O$]; ^{13}C NMR (100 MHz, $CDCl_3$):

δ_C 170.6, 170.3, 169.4, 169.2 (*C*O), 100.8 (C-1), 72.9 (C-3), 71.8 (C-5), 71.4 (C-2), 70.2 [$CH_3(CH_2)_6CH_2O$], 68.6 (C-4), 62.1 (C-6), 31.8, 29.4, 29.3, 29.2, 25.8, 22.6 [$CH_3(CH_2)_6CH_2O$], 20.7, 20.6(3) (CH_3CO), 14.0 [$CH_3(CH_2)_7O$]; Anal. Calcd for $C_{22}H_{36}O_{10}$: C, 57.38; H, 7.88. Found: C, 57.45; H, 7.92.

*5.2.9. Octyl 2,3,4,6-tetra-O-benzoyl-β-D-glucopyranoside (**10**):* White solid, mp 97-100 °C, yield 87%; R_f = 0.67 (*n*-hexane/EA = 2/1); FT-IR (KBr): ν 1723, 1719, 1715, 1710 (CO), 1069 cm^{-1} (pyranose ring); ^{1}H NMR (400 MHz, $CDCl_3$): δ_H 8.04 (d, 2H, J 7.2 Hz, Ar-*H*), 7.98 (d, 2H, J 7.2 Hz, Ar-*H*), 7.92 (d, 2H, J 7.2 Hz, Ar-*H*), 7.84 (d, 2H, J 7.2 Hz, Ar-*H*), 7.51-7.58 (m, 3H, Ar-*H*), 7.28-7.49 (m, 9H, Ar-*H*), 5.93 (t, 1H, $J_{3,4}$ 9.6 Hz, H-3), 5.69 (t, 1H, $J_{4,5}$ 9.6 Hz, H-4), 5.54 (dd, 1H, $J_{2,3}$ 9.8 Hz, H-2), 4.85 (d, 1H, $J_{1,2}$ 8.0 Hz, H-1), 4.66 (dd, 1H, $J_{6a,6b}$ 12.0, $J_{5,6a}$ 3.2 Hz, H-6a), 4.53 (dd, 1H, $J_{5,6b}$ 5.2 Hz, H-6b), 4.17 (ddd, 1H, H-5), 3.94 [dt, 1H, J 9.6 and 6.0 Hz, $CH_3(CH_2)_6CH_AH_BO$], 3.56 [dt, 1H, J 9.6 and 6.5 Hz, $CH_3(CH_2)_6CH_AH_BO$], 1.49-1.58 [m, 2H, $CH_3(CH_2)_5CH_2CH_2O$], 1.04-1.25 [br m, 10H, $CH_3(CH_2)_5CH_2CH_2O$], 0.85 [t, 3H, J 6.8 Hz, $CH_3(CH_2)_7O$]; ^{13}C NMR (100 MHz, $CDCl_3$): δ_C 166.2, 165.9, 165.2, 165.1 (*C*O), 133.4, 133.2, 133.1, 133.0, 129.9, 129.8, 129.7(2), 129.6, 129.5, 128.9(2), 128.4, 128.3(3) (Ar-*C*), 101.3 (C-1), 73.0 (C-3), 72.2 (C-5), 72.0 (C-2), 70.4 [$CH_3(CH_2)_6CH_2O$], 70.0 (C-4), 63.3 (C-6), 31.7, 29.4, 29.2, 29.1, 25.8, 22.6 [$CH_3(CH_2)_6CH_2O$], 14.0 [$CH_3(CH_2)_7O$]; Anal. Calcd for $C_{42}H_{44}O_{10}$: C, 71.17; H, 6.26. Found: C, 71.25; H, 6.28.

5.3. Evaluation of in vitro antimicrobial activities

In the present study, five human pathogenic bacteria were used as test organisms, to detect the antibacterial activities of different OBG esters as shown in Table 9. Among these human pathogens two was Gram-positive and five were Gram-negative. *In vitro* antifungal activities of the synthesized OBG derivatives were investigated against four human pathogenic fungi. The test tube cultures of the bacterial and fungal pathogens were collected from the Microbiology Laboratory, Department of Microbiology, University of Chittagong, Bangladesh.

Table 9. Name of the microorganisms.

Sl.	Strain	Reference	Source
Gram-positive bacteria			
(i)	*Bacillus subtilis*	ATCC 6633	Gastrointestinal tract
(ii)	*Staphylococcus aureus*	ATCC 25923	Clinical strains
Gram-negative bacteria			
(iii)	*Escherichia coli*	ATCC 25922	Clinical isolate
(iv)	*Escherichia coli*	ATCC 8739	Lower gut of animals
(v)	*Pseudomonas aeruginosa*	ATCC 8027	Animal skin
(vi)	*Pseudomonas aeruginosa*	ATCC 27853	Animal skin
(vii)	*Salmonella abony*	NCTC 6017	Natural sugars
Name of the fungi		Type of organism	
(i)	*Aspergillus flavus*	Human pathogenic	
(ii)	*Aspergillus niger*	Human pathogenic	
(iii)	*Candida albicans*	Human pathogenic	
(iv)	*Fusarium solani*	Human pathogenic	

5.3.1. Screening of antibacterial activity

For antibacterial activities test, the disc diffusion method [24] was followed. Dimethyl sulfoxide (DMSO) was used as a solvent for test chemicals and a 2% solution of the compound was used in the investigation. The plates were incubated at 37 °C for 48 h. Proper control was maintained with DMSO without chemicals. Mueller-Hinton (agar and broth) medium was used for culture of bacteria. Each experiment was carried out three times. All the results were compared with the standard antibacterial antibiotic ciprofloxacin (10 μg dw/disc, brand name Ciprocin, Square Pharmaceuticals Ltd., Bangladesh).

5.3.2. Screening of mycelial growth

The antifungal efficacy of the newly synthesized OBG esters (**3-10**) was investigated based on food poisoning technique [25]. Sabouraud (agar and broth, PDA) medium was used for culture of fungi. Linear mycelial growth of fungus was measured after 3~5 days of incubation. The percentage inhibition of radial mycelial growth of the test fungus was calculated as $I = \left\{\frac{(C-T)}{C}\right\} \times 100$

where, I = percentage of inhibition, C = diameter of the fungal colony in control (DMSO), T = diameter of the fungal colony in treatment. The results were compared with standard antifungal antibiotic fluconazole (10 μg dw/mL medium, brand name Flugal® 50, Square Pharmaceuticals Ltd., Bangladesh).

5.4. ADME/T Analysis

We have analyzed ADME/T of all the compounds by using computational approaches. For these calculations, at first, we have drawn all the structures of OBG esters in ChemDraw 18.0 to collect InChI Key, isomeric SMILES and SD file format. Absorption, distribution, metabolism, excretion and toxicity (ADMET) of all the OBG esters were predicted by using AdmetSAR [31] and SwissADME [32] free web tools. SMILES (simplified molecular-input line-entry system) strings were used throughout the process. InChI Key were used to find these compounds in different databases, we found only **9** and **10** in PubChem database [33] as CID 9847074 and 101430141, respectively.

5.5. Molecular Docking and non-bond interaction analysis

Lanosterol 14-alpha demethylase catalyzes C14-demethylation of lanosterol which is important for ergosterol biosynthesis [28]. Inhibition of this enzyme stopped ergosterol synthesis, which further facilitates cell membrane to rapture in microorganisms. Azoles are known as inhibitors of lanosterol 14-alpha demethylase and the crystal structures of their complexes with the bacterial or fungal enzyme were determined previously [34]. Looking for the structural understanding we have docked these new synthetic compounds with lanosterol 14-alpha demethylase and compare docking score and non-bond interaction with bounded itraconazole.

5.5.1. Ligand preparation

After drawing the entire synthetic compounds in ChemDraw 18.0 we have saved all the compounds as SDF format. Further, all the SDF prepared for dataset by using Schrödinger Suite 2013 [35] software. Here, all ligands were minimized in Ligprep2.5 wizard, by applying OPLS 2005 force field. During the minimization, the module Epik 2.2 [36] was utilized to fix the ionization state of the ligand at pH 7.0 ± 2.0. From this analysis, up to 32 possible stereoisomers of each compound were generated and we selected the best conformer with lowest energy for structural understanding.

5.5.2. Protein Preparation

Protein structures for molecular docking were prepared using the protein preparation module of Schrödinger Suite 2013 [35] software, in which the crystal structure is initially assigned proper hydrogen, charges and bond orders. As the main target of the molecular docking was lanosterol 14-alpha demethylase, its crystal structure was retrieved from the RCSB protein data bank (PDB id: 5V5Z; organism: *Candida albicans*). At neutral pH, all hydrogen bonds in the structure were optimized, deleting unnecessary water. Afterwards,

the minimization process was run with the OPLS 2005 force field, considering structural changes of not more than 0.30 Å of RMSD. The active site of the protein was fixed for docking simulation by generating a grid box at the reference ligand binding the protein. Grid generation parameters were kept at default, with a box size of 18 Å × 18 Å × 18 Å, and the OPLS 2005 force field utilized for post minimization. The charge cutoff and van der Waals scaling factor were set to 0.25 and 1.00, respectively [37].

5.5.3. Molecular docking

We carried out extra precision (XP) flexible docking using the Glide module of Schrödinger-Maestro v9.4 [38] which is more sophisticated than SP/HTVS in scoring function [38]. Here, all ligands were treated flexibly, considering the partial charge and van der Waals factor of 0.15 and 0.80, respectively. Minimization was performed to the docked complex after docking using the OPLS 2005 force field. The best-docked pose with lowest Glide score value was recorded for each ligand [37].

Acknowledgements

This work was supported by the Ministry of Education, Bangladesh and BANBEIS [grant no. PS 201660, 2016-17]. One of the authors (P.C.) is indebted to Ministry of Science and Technology for NST fellowship.

References

[1] (*a*) D.D. Dhavale, M.M. Matin, Selective sulfonylation of 4-*C*-hyroxymethyl-β-L-threo-pento-1,4-furanose: Synthesis of bicyclic diazasugars, Tetrahedron 60 (2004) 4275-4281; (*b*) L. Casas-Godoy, J. Arrizon, D. Arrieta-Baez, F.J. Plou, G. Sandoval, Synthesis and emulsifying properties of carbohydrate fatty acid esters produced from *Agave tequilana* fructans by enzymatic acylation, Food Chem. 204 (2016) 437-443; (*c*) MM Matin, Synthesis of D-glucose derived oxetane: 1,2-*O*-isopropylidene-4-(*S*)-3-*O*,4-*C*-methylene-5-*O*-methanesulfonyl-β-L-threo-pento-1,4-furanose, J. Appl. Sci. Res. 4 (2008) 1478-1482.

[2] S. Piccicuto, C. Blecker, J.C. Brohee, A. Mbampara, G. Lognay, C. Deroanne, M. Paquot, M. Marlier, Sugar esters: ways of synthesis and potential applications, Biotech. Agron. Soc. Environ. 5 (2001) 209-219.

[3] K. Hill, O. Rhode, Sugar-based surfactants for consumer products and technical applications, Fett/Lipid, 1 (1999) 25-33.

[4] (*a*) J. Lawandi, S. Rocheleau, N. Moitessier, Regioselective acylation, alkylation, silylation and glycosylation of monosaccharides, Tetrahedron 72 (2016) 6283-6319; (*b*) W. Muramatsu, T. Kawabata, Regioselective acylation of 6-*O*-protected octyl β-

D-glucopyranosides by DMAP catalysis, Tetrahedron Lett. 48 (2007) 5031-5033.

[5] (*a*) M.M. Matin, M.M.H. Bhuiyan, A.K.M.S. Azad, S.C. Bhattacharjee, M.H.O. Rashid, Synthesis and antimicrobial studies of 6-*O*-lauroyl-1,2-*O*-isopropylidene-α-D-gluco-furanose derivatives, Chem. Biol. Interface 4 (2014) 223-231; (*b*) M.M. Matin, M.M.H. Bhuiyan, D.C. Debnath, M.A. Manchur, Synthesis and comparative antimicrobial studies of some acylated D-glucofuranose and D-glucopyranose derivatives, Int. J. Biosci. 3 (2013) 279-287; (*c*) M.M. Matin, M.M.H. Bhuiyan, E. Kabir, A.F.M. Sanaullah, M.A. Rahman, M.E. Hossain, M. Uzzaman, Synthesis, characterization, ADMET, PASS predication, and antimicrobial study of 6-O-lauroylmannopyranosides, J. Mol. Structure 1195 (2019) 189-197.

[6] M.M. Matin, Synthesis and antimicrobial study of some methyl 4-*O*-palmitoyl-α-L-rhamnopyranoside derivatives, Orbital: The Electron. J. Chem. 6 (2014) 20-28.

[7] (*a*) X. Lou, J. O'Brien, G. Henehan, S. Cassidy, Regioselective synthesis of fatty acid esters of methyl α-D-glucopyranoside with dibutyltin dimethoxide method and biological test against *Staphylococcus aureus* and *Salmonella agona*, Asian J. Chem. 22 (2010) 3135-3146; (*b*) A.K.M.S. Kabir, M.M. Matin, M. Ali, M.N. Anwar, Comparative studies on selective acylation and antimicrobial activities of some D-glucofuranose derivatives, J. Bangladesh Aca. Sci. 27 (2003) 43-50; (*c*) A.K.M.S. Kabir, M.M. Matin, M.M.R. Bhuiyan, M.A. Rahim, Synthesis and characterization of some acylated derivatives of D-mannose, Chittagong Univ. J. Sci. 25 (2001) 65-73.

[8] T. Kobayashi, Lipase-catalyzed syntheses of sugar esters in non-aqueous media, Biotechnol. Lett. 33 (2011) 1911-1919.

[9] Microwave in Organic Synthesis, A. Loupy (Ed), Second ed., Wiley-VCH, Weinheim, 2006.

[10] (*a*) M. Therisod, A.M. Klibanov, Regioselective acylation of secondary hydroxyl groups in sugars catalyzed by lipases in organic solvents. J. Am. Chem. Soc. 109 (1987) 3977-3981; (*b*) D.A. MacManus, E.N. Vulfson, Substituent effects on the regioselectivity of enzymatic acylation of 6-*O*-alkylglycopyranosides using *Pseudomonas cepacia* lipase. Carbohydr. Res. 279 (1995) 28l-291.

[11] R. Perez-Tomas, Multidrug resistance: Retrospect and prospects in anti-cancer drug treatment, Current Med. Chem. 13 (2006) 1859-1876.

[12] J. Staron, J.M. Dabrowski, E. Cichon, M. Guzik, Lactose esters: synthesis and biotechnological applications, Crit. Rev. Biotechnol. 0 (2017) 01.

[13] M. Habulin, S. Sabeder, Z. Knez, Enzymatic synthesis of sugar fatty acid esters in organic solvent and in supercritical carbon dioxide and their antimicrobial activity, J Supercrit Fluids 45 (2008) 338-345.

[14] L.R. Beuchat, Comparison of anti-Vibrio activities of potassium sorbate, sodium benzoate, and glycerol and sucrose esters of fatty acids, Appl. Environ. Microbiol. 39 (1980) 1178-1182.

[15] M. Suwa, N. Shirota, H. Michida, Effects of food emulsifiers on spoilage of canned coi tee caused by thermophilic spore forming bacteria, J. Japan Soc. Food Sci. Technol. 33 (1988) 44-51.

[16] M.N. AlFindee, Q. Zhang, Y.P. Subedi, J.P. Shrestha, Y. Kawasaki, M. Grilley, J.Y. Taemoto, C.W.T. Chang, One-step synthesis of carbohydrate esters as antibacterial and antifungal agents, Bioorg. Med. Chem. 26 (2018) 765-774.

[17] D. Xiao, R. Ye, P.M. Davidson, D.G. Hayes, D.A. Golden, Q. Zhong, Sucrose monolaurate improves the efficacy of sodium hypochlorite against *Escherichia coli* O157:H7 on spinach. International Journal of Food Microbiology, 145 (2011) 64-68.

[18] S. de Lamo-Castellvi, W. Ratphitagsanti, V.M. Balasubramaniam, A.E. Yousef, Inactivation of *Bacillus amyloliquefaciens* spores by a combination of sucrose laurate and pressure-assisted thermal processing. J. Food Protec. 73 (2010) 2043-2052.

[19] A. Wagh, S. Shen, F.A. Shen, C.D. Miller, M.K. Walsh, Effect of lactose monolaurate on pathogenic and nonpathogenic bacteria, Appl. Environ. Micro. 78 (2012) 3465-3468.

[20] (*a*) J.J. Kabara, Medium chain fatty acids and esters, in: P.M. Davidson, A.H. Branen, (Eds.), Antimicrobial in Foods, Mercel Dekker, New York, 1993, pp. 307-342; (*b*) P. Nobmann, P. Bourke, J. Dunne, G. Henehan, *In vitro* antimicrobial activity and mechanism of action of novel carbohydrate fatty acid derivatives against *Staphylococcus aureus* and MRSA, J. Appl. Micro., 108 (2010) 2152-2161.

[21] M. Nüchter, B. Ondruschka, W. Lautenschläger, Synthesis of alkylglycosides by microwaves. Synth. Commun. 31 (2001) 1277-1283.

[22] Polysaccharides: Structural Diversity and Functional Versatility, S. Dumitriu (Ed.), Marcel Dekker, New York, **1998**, p 864.

[23] (*a*) S. Kumaresan, V. Senthilkumar, A. Stephen, B.S. Balakumar, GC-MS Analysis and PASS-assisted prediction of biological activity spectra of extract of *Phomopsis* sp. Isolated from *Andrographis paniculata*, World J. Pharmaceut. Res. 4 (2015) 1035-1053; (*b*) M.M. Matin, A.R. Nath, O. Saad, M.M.H. Bhuiyan, S.B.A. Hamid, A.A. Alhadi, F.A. Kadir, M.E. Ali, W.A. Yehye, 2016, Synthesis, PASS-Predication and *in vitro* antimicrobial activity of benzyl 4-*O*-benzoyl-α-L-rhamnopyranoside derivatives, Int. J. Mol. Sci., 17, 1412. https://doi:10.3390/ijms17091412.

[24] (*a*) A.W. Bauer, W.M.M. Kirby, J.C. Sherris, M. Turck, Antibiotic susceptibility testing by a standardized single disk method, Am. J. Clin. Pathol., 45 (1966) 493-496;

(*b*) A.K.M.S. Kabir, M.M.Matin, A.F.M. Sanaullah, M.A. Sattar, M.S. Rahman, Antimicrobial activities of some lyxoside derivatives, Bangladesh J. Microbiol. 18 (2001) 89-95.

[25] A.K.M.S. Kabir, M.M. Matin, M.A.U. Mridha and S.M. Shahed, Antifungal activities of some methyl 6-*O*-trityl-α-D-mannopyranosides, Chittagong Univ. J. Sci. 22 (1998) 41-46.

[26] M.L. Amin, P-glycoprotein inhibition for optimal drug delivery, Drug Target Insights, 7 (2013) 27-34. doi:10.4137/DTI.S12519.

[27] C.A. Lipinski, F. Lombardo, B.W. Dominy, P.J. Feeney, Experimental and computational approaches to estimate solubility and permeability in drug discovery and development settings, Adv. Drug Delivery Rev. 23 (1997) 3-25.

[28] Y. Aoyama, Y. Yoshida, R. Sato, Yeast cytochrome P-450 catalyzing lanosterol 14 alpha-demethylation. II. Lanosterol metabolism by purified P-450(14)DM and by intact microsomes, J. Biol. Chem. 259 (1984) 1661-1666.

[29] M.M. Matin, M.M.H. Bhuiyan, A.K.M.S. Azad, Synthesis and antimicrobial evaluation of some *n*-butyl α- and β-D-glucopyranoside derivatives, RGUHS J. Pharm. Sci. 3 (2013) 53-59. doi:10.5530/rjps.2013.1.8

[30] W.A. Hunt, The effects of aliphatic alcohols on the biophysical and biochemical correlates of membrane function: Biochemical pharmacology of ethanol, in: E. Majchrowicz (Ed.), Adv. Exp. Med. Biol., Plenum Press, New York, 1975, pp 195-210.

[31] H. Yang, C. Lou, L. Sun, J. Li, Y. Cai, Z. Wang, W. Li, G. Liu, Y. Tang, admetSAR 2.0: web-service for prediction and optimization of chemical ADMET properties, Bioinformatics 35 (2019) 1067-1069.

[32] A. Daina, O. Michielin, V. Zoete, 2017, SwissADME: a free web tool to evaluate pharmacokinetics, drug-likeness and medicinal chemistry friendliness of small molecules,Sci. Rep. 7, 42717.

[33] S. Kim, P.A. Thiessen, E.E. Bolton, J. Chen, G. Fu, A. Gindulyte *et al*., PubChem substance and compound databases, Nucleic Acids Res. 44 (2015) D1202-D1213.

[34] G.I. Lepesheva, L. Friggeri, M.R.J.P. Waterman, CYP51 as drug targets for fungi and protozoan parasites: past, present and future, Parasitol. 145 (2018) 1820-1836.

[35] Schrödinger suite 2011-2, Protein preparation wizard, Schrödinger LLC, New York (USA), 2013.

[36] J.C. Shelley, A. Cholleti, L.L. Frye, J.R. Greenwood, M.R. Timlin, M. Uchimaya, Epik: a software program for pK(a) prediction and protonation state generation for drug-like molecules, J. Comput. Aided Mol. Dis. 21 (2007) 681-691.

[37] K. Banerjee, U. Gupta, S. Gupta, G. Wadhwa, R. Gabrani, S.K. Sharma, C.K. Jain, Molecular docking of glucosamine-6-phosphate synthase in Rhizopus oryzae, Bioinfor. 7 (2011) 285-290.

[38] R.A. Friesner, R.B. Murphy, M.P. Repasky, L.L. Frye, J.R. Greenwood, T.A. Halgren, P.C. Sanschagrin, D.T. Mainz, Extra precision glide: docking and scoring incorporating a model of hydrophobic enclosure for protein-ligand complexes, J. Med. Chem. 49 (2006) 6177-6196.

Highlights

- Regioselective dimolar valeroylation of OBG yields mainly 3,6-di-*O*-valeroates
- Reactivity order in OBG at normal temperature is 6-OH > 3-OH > 4-OH,2-OH
- OBG esters are more prone against fungi than bacterial strains
- Alkyl and aryl ester groups enhance antimicrobial efficacy in OBG